Submitted, accepted and published by
Fuel, 2020, 274, 117803

Improving the oxygen demand in biomass CLC using manganese ores

A. Pérez-Astray, T. Mendiara, L. F. de Diego*, A. Abad, F. García-Labiano, M. T. Izquierdo, J. Adánez

Department of Energy and Environment, Instituto de Carboquímica-ICB-CSIC

Miguel Luesma Castán 4, 50018, Zaragoza, Spain

ldediego@icb.csic.es

* Corresponding author:

Phone: + 34 976 733 977;

Fax: +34 976 733 318

Abstract

Negative Emission Technologies (NETs) should be implemented to reach the objectives set by the Paris Agreement to limit the average temperature increment to 2 ºC. One of the options is the development of bioenergy with Carbon Capture and Storage (BECCS) technologies. In this sense, Chemical Looping Combustion (CLC) is one of the most efficient CO_2 Capture technologies both from economical and energy points of view. In CLC, a solid oxygen carrier is used to transfer the oxygen from air to the fuel.

In this work two manganese-based ores were used as oxygen carriers to burn three different types of biomass (pine sawdust and two Spanish agricultural residues) in a 0.5 kW_{th} CLC continuous unit. Operational conditions were varied to evaluate their effect on the CO_2 capture efficiency and the total oxygen demand of the process. Almost 100% of CO_2 capture efficiency was reached working with pine sawdust as well as with almond shells. However, high values of total oxygen demand (10-20 %) were found, which led to consider further technological solutions to increase the combustion efficiency. In this respect, fuel reactor outlet recycling was evaluated as an operational solution to reduce the oxygen demand with good results (about 30% reduction in the total oxygen demand value). NOx and tar formation from the CLC system were also evaluated. There were no NOx emissions during the experimental campaign and low tar content in the fuel reactor outlet gas was reached (0.3-3.2 g/Nm^3), being naphthalene the major tar compound.

Keywords: NETs; BECCS; Chemical Looping Combustion (CLC); biomass; manganese ores; oxygen carrier

1 Introduction

The anthropogenic CO_2 emissions associated to the use of fossil fuels for energy production has altered the CO_2 concentration in the atmosphere increasing the natural greenhouse effect. Based on this evidence, the Intergovernmental Panel on Climate Change (IPCC) has alerted about the dramatic consequences of increasing the Greenhouse Gases (GHG) emissions. This was already reflected in the Paris Agreement, signed by most of the countries in the world in 2015. The agreement pursues to limit the global average temperature increase in less than 2 ºC at the end of the present century [1].

The energy sector is responsible for an important part of the CO_2 emitted to the atmosphere. Only in 2018 about 33.1 Gt_{CO2} were released [2]. In this context, fossil fuels represented about 80% of the primary energy demand in the world. Thus, in order to follow the recommendations in the Paris Agreement, actions should be taken in the energy sector to reduce the dependence on fossil fuels. These actions are mostly based on energy efficiency improvement, deployment of renewable energy and implementation of Carbon Capture and Storage (CCS) technologies. The European Union aimed to increase about 40% the biomass power contribution in 2020 [3], guaranteeing the almost null CO_2 balance and the sustainability of power generation in the lifecycle analysis. Bio Energy with Carbon Capture and Storage (BECCS) combines the use of renewable biofuels, such as biomass, with CCS. The deployment of BECCS technologies would contribute to achieve a negative-CO_2-emission energy sector in the last decades of the present century, and to meet the objectives of the Paris Agreement by removing 22.5 Gt_{CO2} from the atmosphere [4].

Chemical Looping Combustion (CLC) technology has been pointed as one of the most efficient CCS technologies from both energy and economical points of view [5]. The CLC process allows the thermal conversion of the fuel producing a concentrated CO_2 outlet stream, suitable for a long-term storage in safe locations. Figure 1 shows a scheme of the CLC processes. In CLC, a solid oxygen carrier is used to transfer oxygen from the air to the fuel using two interconnected reactors, most commonly fluidized beds. In one of the reactors (fuel reactor), the oxygen carrier is reduced while the fuel is oxidized to CO_2 and H_2O. A CO_2 concentrated stream is generated after steam condensation. In the other reactor (air reactor), the oxygen carrier is oxidized again in air. In the case of solid fuel conversion, the solid fuel enters the fuel reactor where it is devolatilized generating char and volatile matter. A fluidization agent, namely H_2O or CO_2, is used as a gasifying agent of the char produced during devolatilization. The oxygen carrier reacts with the gaseous biomass decomposition products producing H_2O and CO_2.

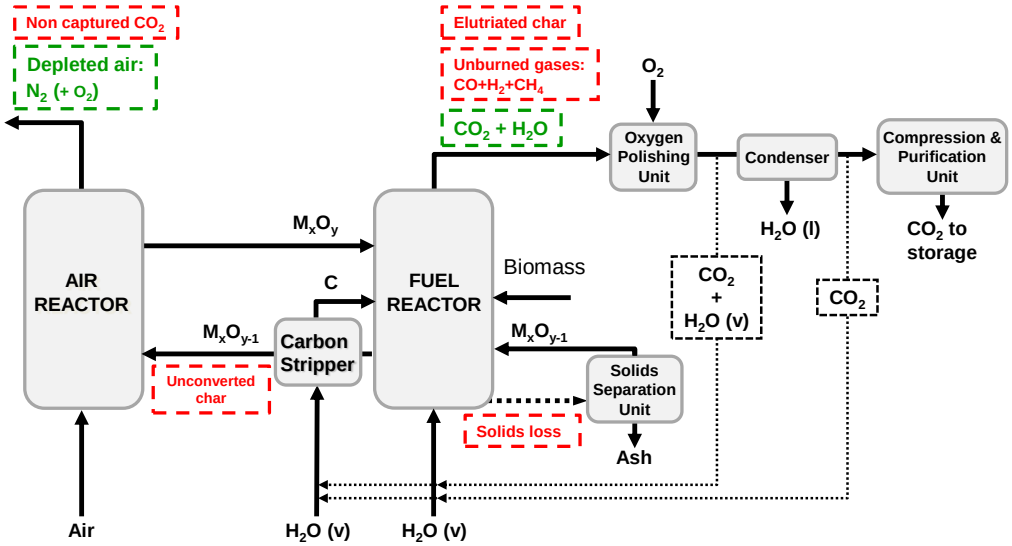

Figure 1. General scheme of a CLC process for solid fuels

The development and testing of potential oxygen carriers is the cornerstone of the CLC technology. Most of the materials developed to date as oxygen carriers are based on nickel, copper, iron and manganese oxides [6], although the use of nickel oxide has been recently disregarded due to its toxicity. Besides, in the case of the combustion of solid fuels, it is especially important to consider the cost of the oxygen carrier to be used in the process since some oxygen carrier losses are expected in the drainage of the solid fuel ashes from the CLC system [7]. In this sense, both iron and manganese oxides would be preferred, due to their large availability, low cost and non-toxic properties. In recent years, intensive research has been conducted to identify both synthetic materials and minerals based on iron and manganese oxides as potential oxygen carriers for the CLC combustion of solid fuels [6]. Research has specifically focused on minerals or industrial residues since they require minimal pretreatment/conditioning and have low production costs [8]. Different iron ores were firstly investigated in the combustion of coal. Many of the research works used ilmenite ($FeTiO_3$) as oxygen carrier. Its good reactivity and mechanical properties converted it in the reference material for solid fuel combustion [6]. Nevertheless, there are other hematite-based minerals with promising characteristics, like that denoted as Tierga ore. Experiments with coal in continuous CLC units demonstrated that it was possible to achieve better combustion efficiencies using Tierga ore when compared under similar conditions to the values obtained with ilmenite [9, 10]. Manganese ores have also attracted attention as oxygen carriers in recent years. They showed better performance than ilmenite in the combustion of coal [11-13] but in many cases lower mechanical properties (soft and prone to attrition) [14].

Focusing on the specific case of biomass combustion, high values of carbon capture efficiency (>90%) were obtained using hematite-based minerals or ilmenite in experimental campaigns in continuous CLC units using different types of biomass [10, 15, 16]. However, in many of these works, low values of combustion efficiencies were reached, which represented total oxygen demands of 20-30 % [17]. Manganese ores from different origins and different characteristics have been also studied in recent years as oxygen carriers for biomass combustion at various laboratory scales due to its high reactivity compared to Fe-based ores. Schmitz et al. [11, 13] tested different manganese ores in a 10 and 100 kW_{th} units using biochar and black wood pellets reaching up to 93.5% combustion efficiency. Pikkarainen and Hiltunen [18] used wood pellets, black pellets and wood char in different tests in a 50 kW_{th} unit with braunite as oxygen carrier. Total oxygen demands between 27 and 31% were obtained for the wood pellets. Our research group performed a screening study in a batch fluidized bed reactor with various manganese oxygen carriers, including manganese ores from South Africa, Gabon and Brazil [19, 20]. Based on both reactivity and attrition rate, two promising manganese ores were identified, one came from South Africa (MnSA) and another from Gabon (MnGBHNE).

Thus, the main objective of the present work was to assess the potential of these manganese ores in the CLC of biomass in order to improve the combustion efficiency of the process and therefore reduce the oxygen demand values previously reported for Fe-based oxygen carriers. To reach this objective, the influence of different operating variables of the process was evaluated. Different types of biomass were used as fuel, including pine sawdust and two Spanish agricultural residues (olive stones and almond shells). Besides the evaluation of more reactive oxygen carriers, the reduction of the total oxygen demand in CLC of biomass was also addressed considering the gas recirculation of the outlet stream from the fuel reactor.

2 Materials and methods

2.1 Materials

Two manganese-based ores were used during the experimental campaign as oxygen carriers. One came from Gabon (hereafter named MnGBHNE) and another one from South Africa (hereafter named MnSA), both supplied by Hidro Nitro Española S.A. The natural ores were crushed and sieved to 100–300 μm, and then thermally treated in air at 800 °C during 2 h to increase their crushing strength. Table 1 presents the main properties of both manganese oxygen carriers. More information about the oxygen carriers can be found elsewhere [19]. A Spanish pine wood biomass (*Pinus sylvestris*) together with two Spanish agricultural residues, olive stones (*Olea europaea*) and almond shells

(*Prunus dulcis*), were selected as fuels because of their high availability [21, 22]. The raw materials were ground and sieved to +500–2000 μm. The main characteristics of these fuels are presented in Table 2, together with the technical standards used in the analyses.

Table 1: Main properties of the manganese ores oxygen carriers.

		MnGBHNE	MnSA
Redox composition (wt.%)[a]	**Mn_3O_4**	67.5	65.6
	Fe_2O_3	10.8	18.6
Crushing strength (N)		1.8	4.6
Air Jet Index (%)		14.4	5.5
Oxygen transport capacity, R_{OC} (%)[a]		5.1	4.7
Porosity (%)		38.7	12.3
Skeletal density (kg/m^3)		2800	3510
BET surface area (m^2/g)		12.3	0.6

[a] Quantified by thermogravimetric analysis [19]

Table 2: Main characteristics of the different types of biomass.

		Pine sawdust	Almond shells	Olive stones
Proximate Analysis (wt%)				
Moisture	(EN 14774-3)	4.2	2.3	9.4
Volatile matter	(EN 15148)	81.0	76.6	72.5
Fixed carbon[a]		14.4	20.0	17.3
Ash	(EN 14775)	0.4	1.1	0.8
Ultimate Analysis (wt%)[b]				
C		51.3	50.2	46.5
H		6.0	5.7	4.8
N		0.3	0.2	0.2
S		0.0	0.0	0.0
O[a]		37.8	40.5	38.3
LHV (kJ/kg)	(EN 14918)	19158	18071	17807
Ω_{sf} (kg O_2/kg biomass)		1.5	1.4	1.2

[a] By difference; [b] Performed in a Thermo Flash 1112

2.2 Experimental set up

Figure 2 presents a scheme of the 0.5 kW_{th} continuous CLC unit used during all the experimental campaign. A detailed description of the unit can be found elsewhere [16] and only a brief description is included here. The unit is based in two bubbling bed reactors connected by loop seals that avoid the mixture of the gases. The upper loop seal also acts as solids reservoir at the fuel reactor entrance. A

conical solids valve is used in the unit for the solids circulation rate control. Besides a diverting valve is used for the solids circulation rate measurement. Various highly efficient cyclones collect the solids materials exiting the reactors. Electric furnaces allow the temperature control in each reactor. The unit is equipped with different temperature and pressure drop sensors connected to a computer where data are registered. A double screw feeder is used to control the solid fuel fed at the botton part of the fuel reactor. The experimental campaign involved more than 160 h of hot fluidization with more than 63 h of biomass combustion.

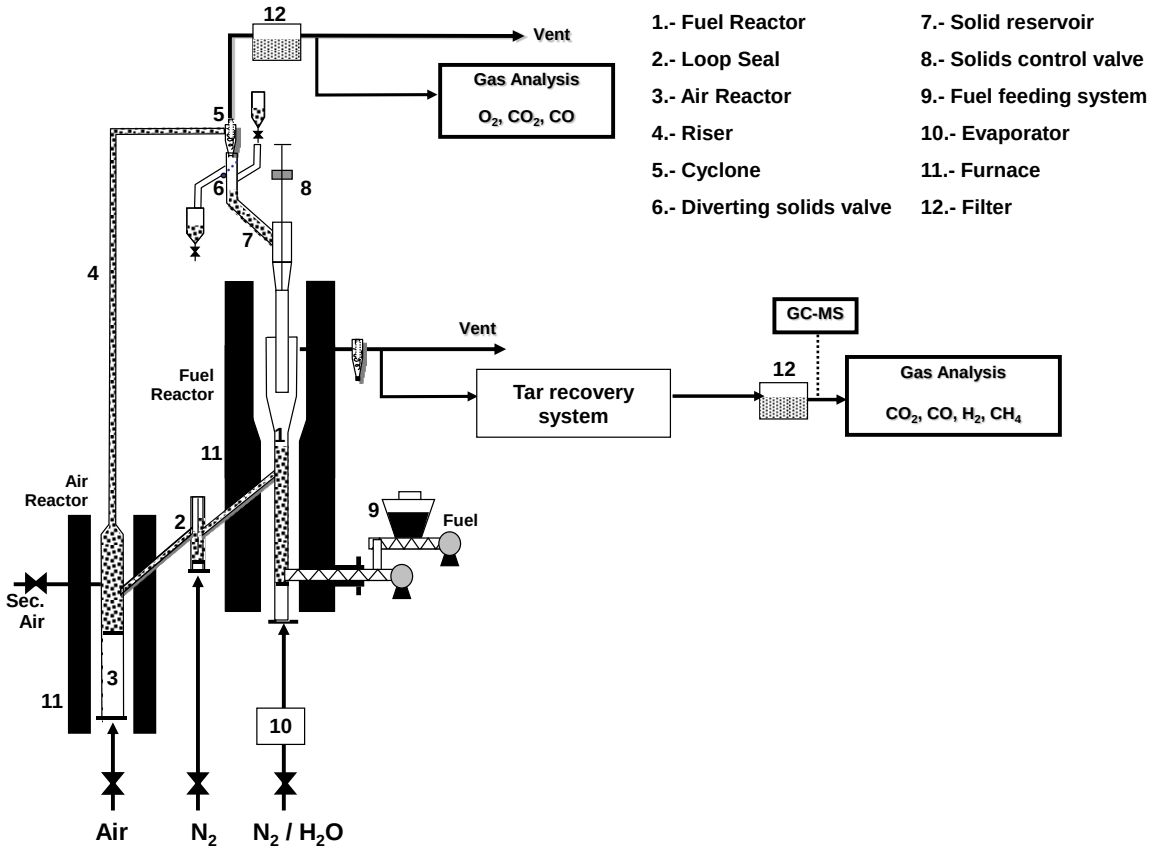

Figure 2. Experimental unit, ICB-CSIC-s1

The flows of fluidizing gas at the inlet of the fuel and air reactors were kept constant at 130 and 1200 l_N/h (STP), respectively, during all the experimental campaign. These flows corresponded to fluidization velocities of about 0.1 m/s in the fuel reactor and 0.5 m/s in the air reactor. The fuel reactor temperature range was varied between 850 and 950 ºC. The temperature in the air reactor was always kept constant at 950 ºC. The solids inventories were about 2.3 kg for the MnGBHNE and 3.0 kg for the MnSA. Tar collection at the fuel reactor outlet was carried out according to the standard protocol [23] and a gas chromatograph coupled to a mass spectrometer was used in the analysis, being naphthalene and phenanthrene chosen for the external calibration procedure.

147 Table 3 presents the experimental series performed with the main operating conditions used in the
148 experimental campaign: 15 tests at steady state operating conditions were carried out with MnGBHNE
149 and 8 with MnSA as oxygen carriers. Previous experiments performed with the same biomasses and
150 with the Fe-based oxygen carrier named as Tierga ore have been also considered for comparison [16].
151 Tierga ore has been previously identified as one of the most reactive Fe-based oxygen carriers.

152 Table 3: Operating conditions used in the experimental campaign with MnGBHNE and MnSA

Test	F.A (-)	Biomass	T_{FR} (ºC)	ϕ (-)	$\dot{m}_{OC}$ (kg/h)	$\dot{m}_{sf}$ (kg/h)	P (W_{th})	m^*_{FR} kg/MW	norm.$\dot{m}_{oc}$ (kg/s)·MW_{th}
MnGBHNE									
GB1	H_2O	Pine	950	1.0	3.8	0.128	680	650	**1.6**
GB2	H_2O	Pine	935	2.0	7.2	0.120	639	605	**3.1**
GB3	H_2O	Pine	945	3.5	12.0	0.117	623	670	**5.4**
GB4	H_2O	Pine	920	3.5	12.0	0.117	623	685	**5.4**
GB5	H_2O	Pine	925	3.5	12.0	0.117	623	675	**5.4**
GB6	H_2O	Pine	**855**	2.0	7.2	0.120	639	590	3.1
GB7	H_2O	Pine	**890**	1.8	7.2	0.135	718	555	2.8
GB8	H_2O	Pine	**900**	2.0	7.2	0.120	639	625	3.1
GB9	H_2O	Olive	**900**	1.9	6.2	0.132	610	700	2.8
GB10	H_2O	Almond	**905**	1.9	6.5	0.124	617	675	2.9
GB11	H_2O	Almond	**940**	1.5	5.0	0.124	617	650	2.3
GB12	**CO_2**	Pine	**900**	2.9	9.7	0.115	612	665	4.4
GB13	**CO_2**	Pine	**910**	2.9	9.8	0.115	612	775	4.5
GB14	**CO_2**	Pine	**915**	2.7	9.8	0.123	655	715	4.2
GB15	**CO_2**	Pine	**950**	3.3	12.4	0.128	681	520	5.0
MnSA									
SA1	CO_2	Pine	**890**	2.2	8.4	0.120	639	960	3.7
SA2	CO_2	Pine	**900**	2.4	9.2	0.120	639	965	4
SA3	CO_2	Pine	**905**	1.9	7.2	0.120	639	970	3.1
SA4	CO_2	Pine	**910**	2.4	9.2	0.120	639	965	4
SA5	CO_2	Pine	**910**	2.6	9.7	0.120	639	965	4.2
SA6	CO_2	Pine	**925**	2.7	10.2	0.120	639	970	4.4
SA7	CO_2	Pine	**925**	2.5	9.6	0.120	639	965	4.2
SA8	CO_2	Pine	**945**	2.4	9.1	0.120	639	965	4

153

154 **2.3 Data evaluation**

155 To analyze the effect of different operating variables on the performance of both manganese minerals
156 as oxygen carriers, the CO_2 capture efficiency (η_{CC}) and the total oxygen demand (Ω_T) have been

selected as the key parameters. In their calculation, the tar measured at the fuel reactor outlet was not included since its contribution is very low (< 1%).

The CO_2 capture efficiency (η_{cc}) evaluates the CO_2 already captured as a fraction of the produced carbon gases.

$$\eta_{CC} = 1 - \frac{F_{CO_2,outAR}}{F_{CO_2,outFR}+F_{CH_4,outFR}+F_{CO,outFR}+F_{CO_2,outAR}} \quad (1)$$

The total oxygen demand (Ω_T) is the fraction of oxygen needed for the combustion of all the unburned compounds produced and the oxygen needed for the complete combustion of the introduced solid fuel.

$$\Omega_T = \frac{4F_{CH_4,outFR}+F_{CO,outFR}+F_{H_2,outFR}}{\frac{1}{M_O}\Omega_{sf}\dot{m}_{sf}} \quad (2)$$

The oxygen to fuel molar ratio (ϕ) relates the oxygen transferred by the oxygen carrier from the air reactor to the fuel reactor with the oxygen needed for the fuel complete combustion.

$$\phi = \frac{\dot{m}_{OC}\cdot R_{OC}}{\dot{m}_{sf}\cdot\Omega_{sf}} \quad (3)$$

In relation with the ϕ value, the normalized solid circulation rate (norm.$\dot{m}_{oc}$) is defined as the solids circulation rate normalized per MW_{th}.

Finally, carbon mass balances were carried out and the deviations were below 5% in all tests.

3 Results and discussion

3.1 Evaluation of MnGBHNE as oxygen carrier

3.1.1 Influence of the normalized solids circulation rate (norm.$\dot{m}_{oc}$)

The solids circulation rate normalized per MW_{th} is related to the amount of oxygen available for combustion in the fuel reactor. The influence of this parameter was addressed in tests G1-G5. Figure 3 shows the CO_2 capture efficiency and the total oxygen demand at various normalized solids circulation rates for the MnGBHNE burning pine sawdust and using H_2O as gasifying agent at a fuel reactor temperature about 940 ºC.

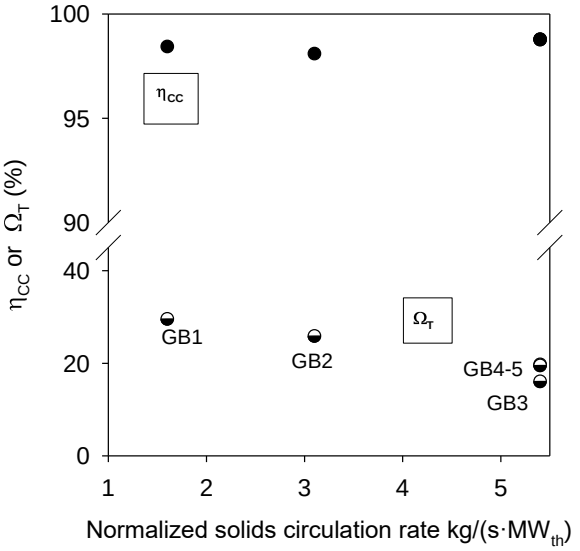

Figure 3. CO_2 capture efficiency and total oxygen demand for different normalized solids circulation rates. Fuel reactor temperature ~940ºC, Biomass: pine sawdust, Gasifying agent: H_2O.

Although the increase in the solids circulation rate implies a decrease in the average residence time of solids in the fuel reactor, the CO_2 capture efficiency seems to be not affected by the normalized solids circulation rate since very high values (>98%) were obtained at any of the conditions tested. This can be due to the high reactivity of the biomass char. However, the total oxygen demand decreased when the normalized solids circulation rate increased, reaching a value about 20% with 5.4 kg/(s·MW$_{th}$), corresponding to ϕ = 3.5. A higher solids circulation rate implies higher oxygen supply in the fuel reactor, decreasing the total oxygen demand values.

3.1.2 Influence of the fuel reactor temperature.

Figure 4 presents the results corresponding to the evaluation of the effect of the fuel reactor temperature (tests GB6 to GB15) on both the CO_2 capture efficiency (η_{CC}) and the total oxygen demand (Ω_T) using the three biomasses (pine, olive stone and almond shell). These experiments were done using steam as well as CO_2 as fluidizing agents. The values of normalized solids circulation rates of the experiments were close to 3 kg/(s·MW$_{th}$) and 4.5 kg/(s·MW$_{th}$), respectively. Also, previous experimental results obtained with the Tierga ore are presented (open symbols) to facilitate the comparison between both oxygen carriers.

The CO_2 capture efficiencies reached, showed in Figure 4(A), with the MnGBHNE oxygen carrier increased with the fuel reactor temperature in the temperature range between 855 and 950 ºC and were higher than 95% at temperatures higher than 880 ºC regardless the biomass and the fluidizing

agent used. It should be here reminded that these results were obtained in the absence of a carbon stripper in the 0.5 kW_{th} unit. The CO_2 capture efficiency values working with pine as fuel were similar to those obtained working with Tierga ore as oxygen carrier. However, higher CO_2 capture efficiencies were reached in the experiments with olive stones and almond shells working with MnGBHNE than working with Tierga ore. This different behaviour would indicate that the conversion of biomass char would be more favoured when MnGBHNE is used as oxygen carrier, as it has been previously reported using coal as fuel [12]. Figure 4(B) shows the values obtained for the total oxygen demand with the different types of biomass. Results working with MnGBHNE showed a clear tendency of the total oxygen demand to decrease with the increase in the fuel reactor temperature. Nevertheless, the oxygen demand values reached were in line to those previously reported for Tierga ore working under similar conditions [16].

Regarding the influence of gasifying agent, similar trends were obtained in both cases when steam or CO_2 were used as gasifying agents. So, it can be concluded that the use of CO_2 would be preferred for working with the MnGBHNE material since in the operation at higher scale recirculated CO_2 from the fuel reactor outlet could be used as gasifyig agent, with the corresponding energy saving associated to steam generation.

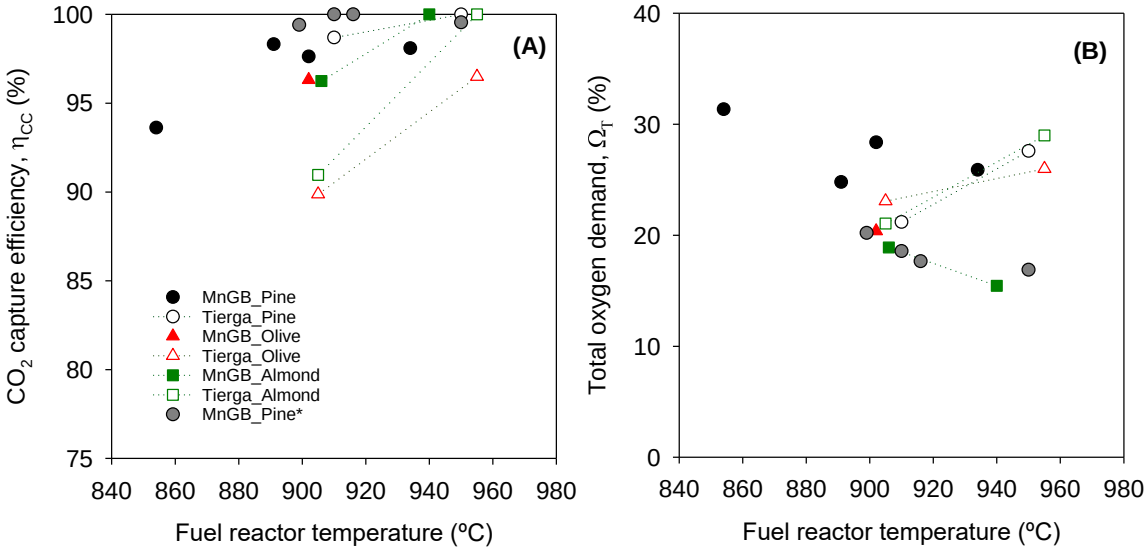

Figure 4. (A) CO_2 capture efficiency and (B) total oxygen demand at different fuel reactor temperatures using MnGBHNE as oxygen carrier. (*CO_2 as fluidizing agent)

Figure 5 shows the contribution to the total oxygen demand value of the different unburnt compounds (H_2, CO and CH_4) measured at the fuel reactor exit for the experiments performed with pine and the

two oxygen carriers under similar operating conditions. As it can be seen, the partial oxygen demands for CO and CH_4 were similar at comparable normalized solids circulation rates, 3.1-3.6 kg/(s·MW_{th}), with both oxygen carriers. A slightly smaller contribution to the total oxygen demand of the H_2 partial demand is observed in the experiments with MnGBHNE in comparison to Tierga.

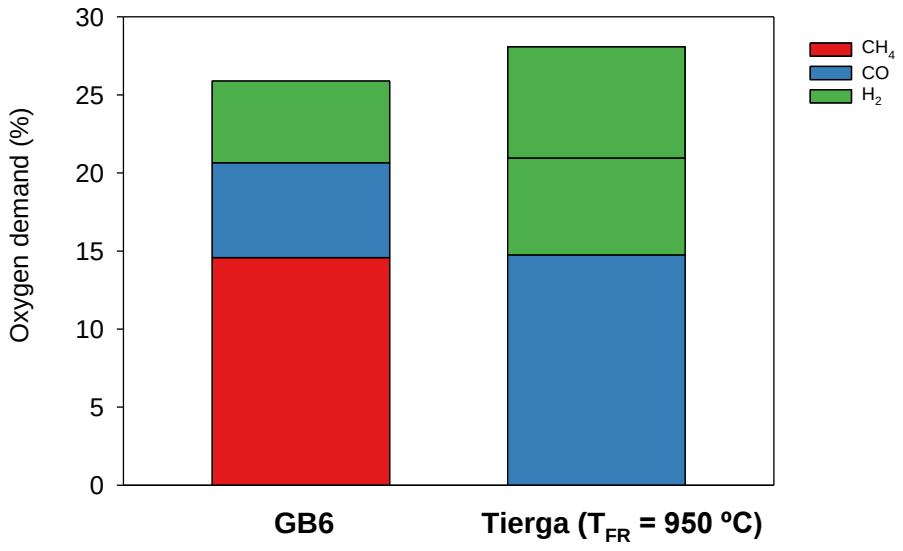

Figure 5. Comparison of partial oxygen demand for H_2, CO and CH_4 at similar operating conditions using Tierga and MnGBHNE as oxygen carriers in experiments with pine.

From the evaluation made in the experimental campaign involving MnGBHNE and the subsequent comparison performed with previous results obtained with Tierga ore under similar conditions, it can be concluded that both carriers performed similarly in CLC of biomass and no clear advantage of one carrier over the other was found.

3.2 Evaluation of MnSA as oxygen carrier

As it is shown in Table 3, experiments were conducted using MnSA as oxygen carrier and pine as fuel at different fuel reactor temperatures (SA1-SA8), using CO_2 as gasifying agent. Figure 6 shows the CO_2 capture efficiencies and the total oxygen demands obtained with both MnGBHNE and MnSA for various fuel reactor temperatures and using normalized solids circulation rates between 3.1-5.0 kg/(s·MW_{th})

Regarding the CO_2 capture efficiency values in Figure 6(A), no differences were observed between both oxygen carriers. Regardless the fuel reactor temperature both manganese ores reached values of CO_2 capture efficiency higher than 97% in this CLC unit without a carbon stripper. Figure 6(B) shows how the total oxygen demand decreased with the fuel reactor temperature for both manganese

ores. Lower oxygen demands up to 10% were obtained with MnSA for similar values of norm.$\dot{m}_{oc}$. Therefore, MnSA can be considered a better alternative for biomass CLC than MnGBHNE or Tierga ore.

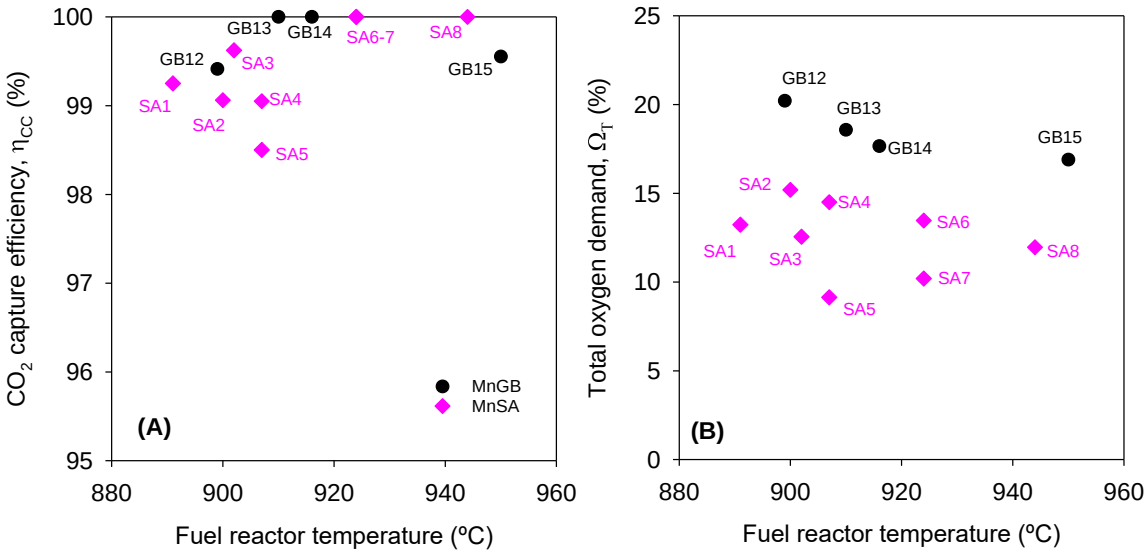

Figure 6. (A) CO_2 capture efficiency and (B) total oxygen demand working with MnGBHNE and MnSA at different fuel reactor temperatures burning pine sawdust. norm.$\dot{m}_{oc}$ = 3.1-5.0 kg/(s·MW_{th})

Figure 7 compares the partial contributions to the total oxygen demand made by each of the unburnt gases in the experiments with both MnGBHNE and MnSA for the fuel reactor temperature of 910 ºC (GB13 and SA5) and 950 ºC (GB15 and SA8) and normalized solids circulation rate about 4 kg/(s·MW_{th}). For both oxygen carriers, the major contribution to the oxygen demand is that coming from unburned methane, followed by CO. However, the contribution of all unburt gases in the case of MnSA is clearly diminished compared to that found for MnGBHNE.

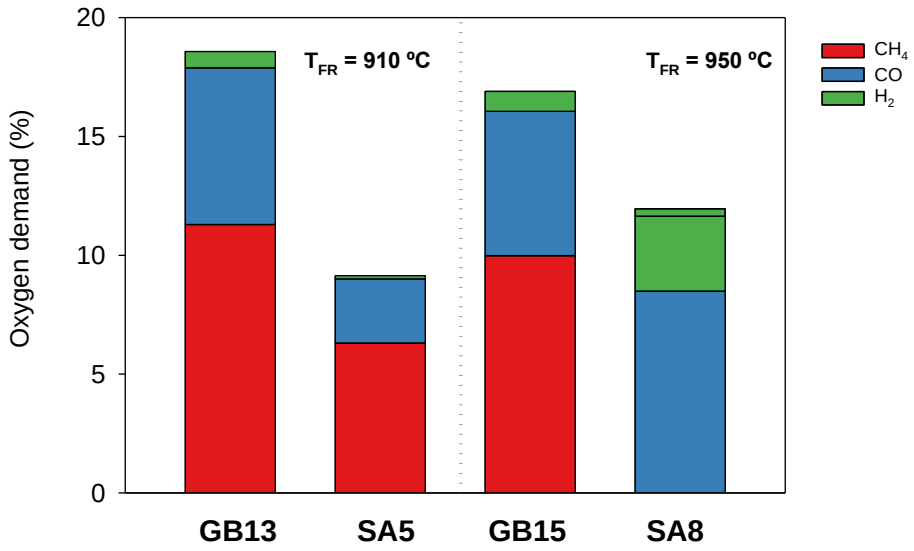

Figure 7. Partial oxygen demand for CH_4, H_2, and CO using MnGBHNE and MnSA as oxygen carriers in experiments with pine sawdust. norm.$\dot{m}_{oc} \approx 4$ kg/(s·MW_{th}).

3.3 Measures to decrease the oxygen demand in biomass CLC

As it has been also observed in the present work, one of the main problems found in the performance of CLC of biomass is the high values obtained for the total oxygen demand [17]. These high values are associated to the high volatile content of biomass when compared to other fuels such as coal. The existence of an elevated amount of unburned products at the fuel reactor outlet makes necessary the incorporation of a oxygen polishing step to complete the combustion. This oxygen polishing represents an important energy penalization for the CLC process and therefore it should be either minimized or even avoided [6]. Several strategies have been proposed in literature to minimize the oxygen polishing step [24]. One of them is the use of highly reactive oxygen carriers. A higher reactivity of the oxygen carrier would facilitate the combustion of H_2, CO and CH_4 in the fuel reactor and would decrease the total oxygen demand. This strategy has been already considered in section 3.2 of the present work, with the testing of MnSA. However, it is already known that not only the reactivity of the oxygen carrier can make the difference in the final value of the oxygen demand. There are other factors associated to the contact between unburned gases and oxygen carrier particles that would also significantly contribute to the oxygen demand decrease. Gayán et al. [24] recently proposed different technological solutions to decrease the oxygen demand, such as the use of a second fuel reactor, the feed of the solid fuel to the carbon stripper or the recirculation of part of the fuel reactor outlet stream. Some of these technological alternatives have been already tested. At Hamburg University of Technology, a

two-stage bubbling bed fuel reactor system in a 25 kW_{th} CLC unit was commissioned and tested [25]. The two stages were separated by a gas distributor placed between the two beds. German hard wood biomass was used as fuel and a copper-based metal oxide, CuO/Al_2O_3, as oxygen carrier. The biomass was fed to the lower stage of the fuel reactor and was gasified there. The gaseous gasification products (H_2, CO and CH_4) rose to the second stage and reacted with freshly oxidized oxygen carrier particles, thus facilitating their combustion. Almost complete combustion of biomass gasification products was achieved in the experiments since the oxygen demand values reported were as low as 1.6%. The effect on the oxygen demand of splitting the fuel reactor into several fluidized beds consecutively placed was also considered in another two 1-2 kW_{th} continuous CLC units [26, 27]. Yan et al. [26] tested a two-step fuel reactor consisting of two spout-fluidized beds using hematite as oxygen carrier. The fuel (sewage sludge) was fed in the bed at the bottom and then gasified. The combustible gases released reacted afterwards in the second bed with oxidized oxygen carrier particles returning from the air reactor. To evaluate the effect of the second bed, the authors defined the combustion compensation efficiency, which calculated the degree of conversion of the combustible gases in the second step of the fuel reactor. They found that this value increased with temperature, reaching values of 50% at 900ºC, the highest temperature tested. Recently, Jiang et al. [27] built a fuel reactor with four gas distributors that divided the reaction chamber into five chambers which were bubbling fluidized beds. In this case, the oxygen carrier particles (Australian hematite) went up with the fuel (sawdust/rice husk) through gas distributors. The conversion of gasification products was significantly improved and no hydrogen was found at the fuel reactor outlet.

In the present work, another of the technological options for oxygen demand reduction has been considered. It was evaluated the effect of the gas recirculation of the fuel reactor outlet stream to the fuel reactor. The methodology used for this purpose was to simulate a recycled stream and to analyze the behavior of the different unburned compounds (i.e H_2, CO and CH_4). For that, tests identified in Table 3 as GB13 and SA5 were selected and individual flows of each unburned compound corresponding to gas concentrations from 0-10% in the inlet stream were introduced while the total flow at the fuel reactor inlet was kept constant at 130 l_N/h. Knowing the amount of gas introduced and the gas concentrations before and after the gas introduction, it was estimated for each of the introduced gases the degree of conversion (χ) in the fuel reactor, which are shown in Table 4. Hydrogen was completely converted regardless the molar flow introduced to the fuel reactor. In the

case of CO and CH_4, conversions about 80% and 70%, respectively, were reached for the different molar flows of each compound.

Table 4. Conversion χ (%) reached for each recirculated gas into the fuel reactor at 910 ºC

Recirculated gas	MnGBHNE χ (%)	MnSA χ (%)
H_2	100	100
CO	81	78
CH_4	67	70

After the experimental tests, it was simulated the behavior of a CLC unit with different gas recirculations (R), see Figure 8. To do this, it was assumed that the flow of stream 1 was constant and it was the sum of the stream 3 and the fed flow of CO_2. Dry recycle (stream 3) was assumed. The recirculation (R) was defined as the percentage of the outlet stream 2 being recycled to the fuel reactor (stream 3). For the simulation, the iterative scheme shown in Figure 9 was used. The iterative process started considering the composition of stream 3 to be the same as that of stream 2 when recirculation was R=0%. Then, a value of R was simulated and the molar flows of each component of stream 3 and stream 1 were calculated. The value of χ in Table 4 for each gaseous compound was considered in order to recalculate the composition in the new stream 2. These values were compared to those calculated in the previous iteration. When the molar flows were similar in both iterations, the iterative process was stopped and the total oxygen demand at the fuel reactor outlet calculated. If they were not similar, a new iteration was done.

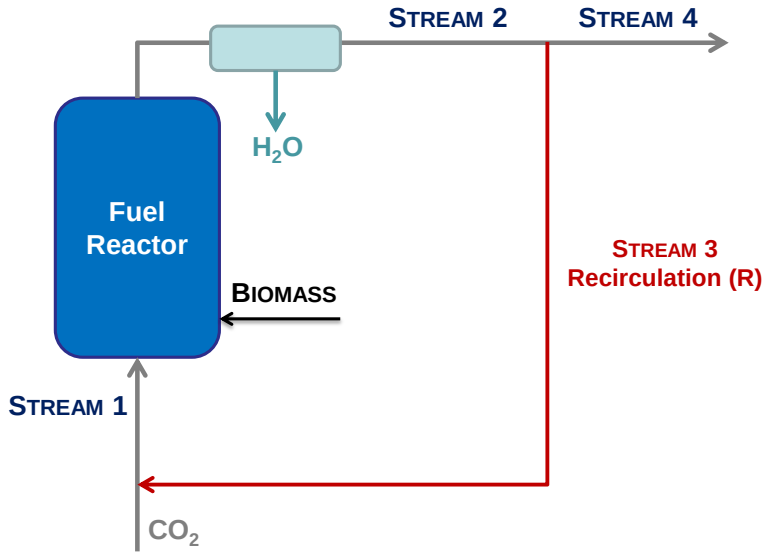

Figure 8. Fuel reactor outlet recycling scheme

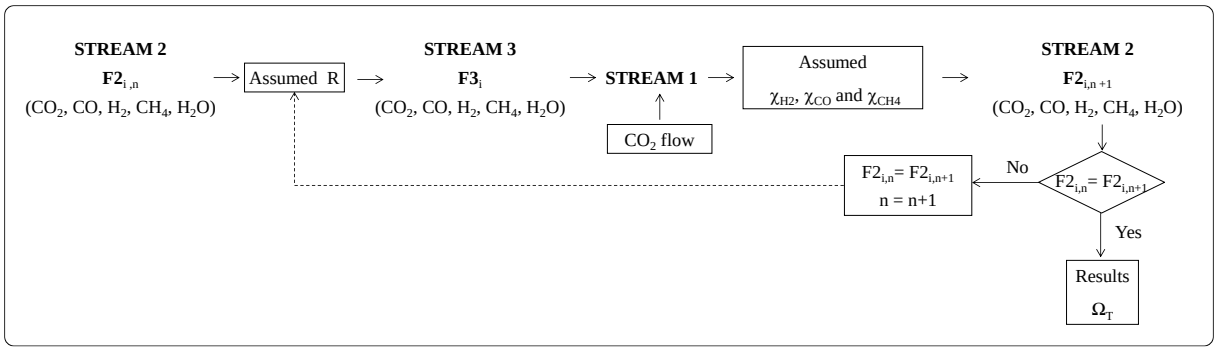

Figure 9. Scheme followed to simulate the gas recirculation to the fuel reactor.

The simulation was carried out for a molar $CO_2/C_{biomass}$ ratio ~ 1.2 (calculated for a R=0%), similar to the ratio used in the experiments GB13 and SA5 and assuming in the first iteration the gas outlet composition of those tests. Figure 10 represents the total oxygen demand values as a function of the gas recirculation for both MnGBHNE and MnSA oxygen carriers in the combustion of pine sawdust. As it can be observed, the total oxygen demand is reduced when the gas recirculation is increased. In the limit case, that is, when the fuel reactor is fluidized with only recirculated gas ($F_{stream\ 1} = F_{stream\ 2}$, R~50%), values close to 30% of total oxygen demand reduction were observed for both oxygen carriers, pointing to the promising possibilities of this technical improvement.

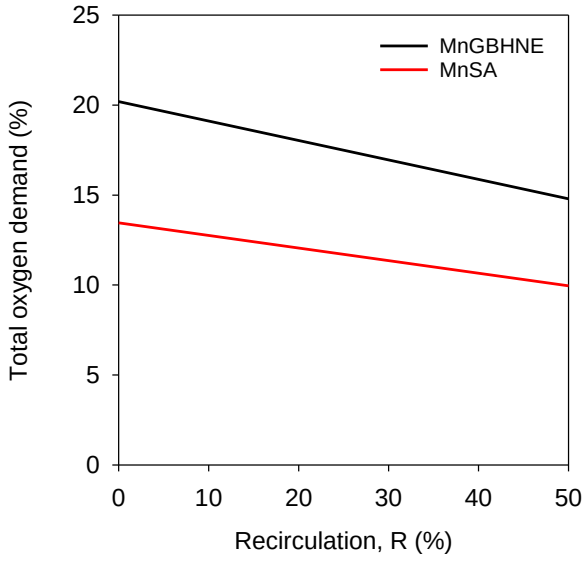

Figure 10. Effect on total oxygen demand of outlet gas recycling into the fuel reactor

3.4 NO_x and tar emissions during biomass combustion

Previous studies with biomass fueled CLC using the Tierga ore as oxygen carrier demonstrated the lower formation of NO_x compared with the conventional biomass combustion. Most of the fuel-N appeared as N_2 at the fuel reactor outlet with only little presence of NO at the air reactor [28]. Similar conclusions were obtained in the present work with both MnGBHNE and MnSA oxygen carriers. The

high CO_2 capture efficiencies obtained, shown in Figures 3, 4 and 6, revealed a high char conversion in the fuel reactor and, therefore, almost no unconverted char reached the air reactor. Thus, no NO_x emissions from the air reactor were detected during the present experimental campaign.

Regarding the amount of NO_x present in the fuel reactor outlet stream, the value of the NO_x/C molar ratio was evaluated in order to determine whether this ratio was lower than 280 ppm that is the maximum recommended value for CO_2 concentrated streams to be transported and stored [29]. As it can be seen in Table 5, in all of the experiments with MnGBHNE and MnSA, the NO_x/C ratios were well below 280 ppm and decreased as fuel reactor temperature increased. Similar NO_x/C values were obtained for pine sawdust and olive stones and slightly lower for almond shells under similar experimental conditions (GB6, GB9 and GB10). Comparing the results obtained with both MnGBHNE and MnSA, it can be concluded that no important differences were observed between both oxygen carriers.

Table 5. NO_x/C ratios obtained under different experimental conditions

Test	Gasifying agent	Biomass	T_{FR} (ºC)	ϕ	NO_x/C (ppm)
GB6	H_2O	Pine sawdust	855	2.0	218
GB9	H_2O	Olive stones	900	1.9	213
GB10	H_2O	Almond shells	905	1.9	160
GB14	CO_2	Pine sawdust	915	2.7	78
GB3	H_2O	Pine sawdust	945	3.5	67
SA1	CO_2	Pine sawdust	890	2.2	97
SA5	CO_2	Pine sawdust	910	2.6	102
SA7	CO_2	Pine sawdust	925	2.5	96
SA8	CO_2	Pine sawdust	945	2.4	50

Another of the emissions from biomass CLC systems is tar. Previous studies with Tierga ore analysing the tar presence in biomass CLC identified naphthalene as the major compound in the tar measured at different operating conditions with pine sawdust. A total tar amount of 2.5-4.3 g/Nm^3 in the temperature range 950-980 ºC was reported [28]. As it can be seen in Figure 11, naphthalene was also the major tar compound determined in the experiments with MnGBHNE and MnSA and pine sawdust as fuel.

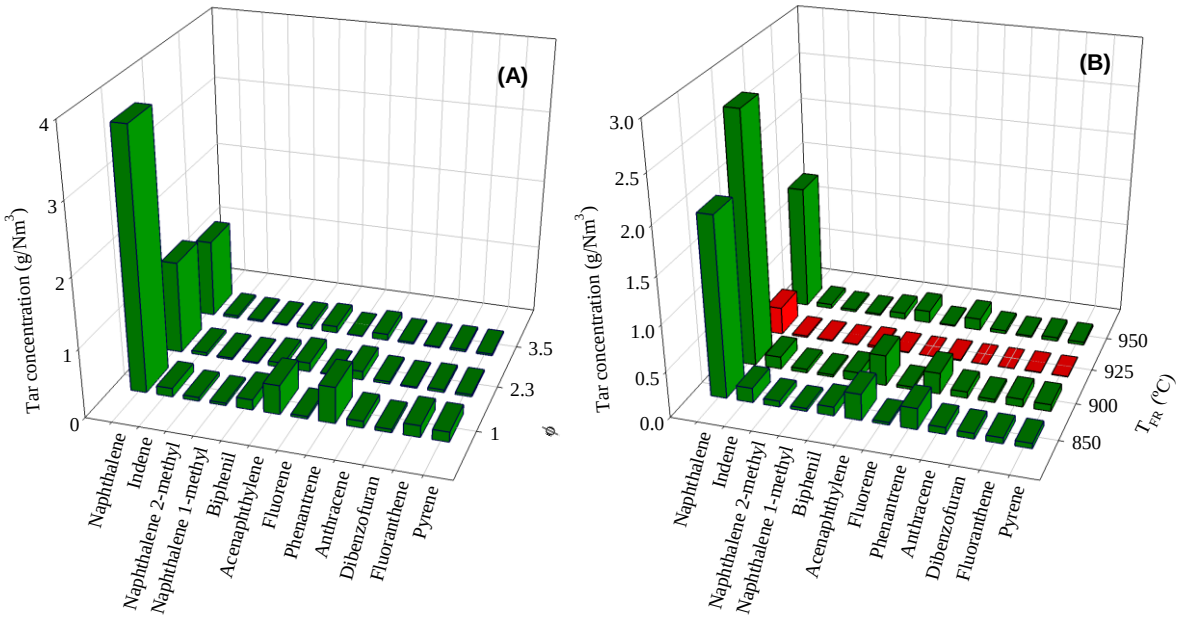

Figure 11. Tar composition as a function of (A) the oxygen to fuel ratio (ϕ) and (B) the fuel reactor temperature in the experiments with MnGBHNE (green bars) and MnSA (red bars) burning pine sawdust.

Figure 11(A) shows that the increase of the oxygen carrier to fuel ratio, ϕ, and therefore, the increase of the oxygen availability in the fuel reactor, decreased the tar concentration. A minimum tar concentration of 1.6 g/Nm^3 was reached at 950 ºC and ϕ =3.5 with MnGBHNE. Also, it can be observed in Figure 11 (B) important differences in the total amount of tar measured between the two oxygen carriers. Values about 1.9-3.2 g/Nm^3 were measured at ϕ~2-3 with MnGBHNE, similar to those found with Tierga ore. Nevertheless, values as low as 0.3 g/Nm^3 were reached working with MnSA under similar conditions.

4 Conclusions

Two manganese ores (MnGBHNE and MnSA) were used as oxygen carriers in a continuous 0.5 kW_{th} prototype burning three different biomasses: pine sawdust, olive stones and almond shells. CO_2 capture efficiency values higher than 95% were obtained with both oxygen carriers in most of the experimental operating conditions, but the oxygen demand values were lower for MnSA than for MnGBHNE. Working with MnSA, the oxygen demands reached values as low as 10%, which are

significant lower than those usually determined for ores. So, this manganese mineral can be thought as an interesting oxygen carrier for further scale up.

For further oxygen demand decrease, the recycling into the fuel reactor of its gas outlet stream was simulated. Simulation results indicated that it is possible to reach an oxygen demand reduction up to 30% working with any of the manganese ores.

In the air reactor, NOx emissions were not detected during the experimental campaign, and in the fuel reactor the values of the NOx/C molar ratio were lower than 280 ppm that is the maximum recommended value for CO_2 concentrated streams to be transported and stored.

Naphthalene was the major tar compound measured at different operating conditions with pine sawdust as fuel, and a total tar concentration value as low as 0.3 g/Nm^3 was reached working with MnSA ore.

Acknowledgements

This work was supported by ENE2017-89473-R AEI/FEDER, UE. A. Pérez-Astray thanks the Spanish Ministry of Economy and Competitiveness (MINECO) for the BES-2015-074651 pre-doctoral fellowship co-financed by the European Social Fund. T. Mendiara thanks for the "Ramón y Cajal" post-doctoral contract awarded by MINECO. The authors also thank Hidro Nitro Española S.A. for providing the solid materials used in this work.

Nomenclature

F_i	flow of compound *i* (mol/s)
M_i	Atomic or molecular weight of i element or compound (kg/mol)
$\dot{m}_{OC}$	solids circulation flow rate (kg/s)
$\dot{m}_{sf}$	mass flow of solid fuel fed (kg/s)
m^*_{FR}	specific solids inventory in the fuel reactor (kg/MW$_{th}$)
$norm.\dot{m}_{oc}$	normalized solids circulation flow rate kg/(s·MW$_{th}$)
P	thermal power (W$_{th}$)
R_{OC}	oxygen transport capacity (kg oxygen per kg oxygen carrier)
T	temperature (ºC)

Greek symbols

ϕ	oxygen carrier-to-fuel ratio (-)
η_{CC}	CO_2 capture efficiency (%)
Ω_{sf}	oxygen demand of the solid fuel (kg oxygen per kg solid fuel)
Ω_T	total oxygen demand (%)

5 References

[1] ONU United Nations Framework Convention for Climate Change. The Paris Agreement. http://unfccc.int/paris_agreement/items/9485.php.

[2] IEA *Global Energy and CO_2 Status report*; Paris (France), 2019.

[3] IRENA *Global Energy Transformation: A roadmap to 2050*; Abu Dhabi, 2018.

[4] Fajardy M, Koeberle A, Mac Dowell N. BECCS deployment: a reality check. Grantham Inst. Brief Pap. 28. Imp. Coll. London 2019;1-13.

[5] IPCC *IPCC special report on carbon dioxide capture and storage*; Cambridge, UK, 2005.

[6] Adánez J, Abad A, Mendiara T, Gayán P, de Diego L F, García-Labiano F. Chemical looping combustion of solid fuels. Prog Energy Combust Sci 2018;65:6-66.

[7] Adánez J, Abad A. Chemical-looping combustion: Status and research needs. Proceedings of the Combustion Institute 2019;37:4303-17.

[8] Matzen M, Pinkerton J, Wang X, Demirel Y. Use of natural ores as oxygen carriers in chemical looping combustion: A review. Int J Greenh Gas Con 2017;65:1-14.

[9] Mendiara T, de Diego L F, García-Labiano F, Gayán P, Abad A, Adánez J. On the use of a highly reactive iron ore in Chemical Looping Combustion of different coals. Fuel 2014;126:239-49.

[10] Linderholm C, Schmitz M. Chemical-looping combustion of solid fuels in a 100 kW dual circulating fluidized bed system using iron ore as oxygen carrier. J Environ Chem Eng 2016;4:1029-39.

[11] Schmitz M, Linderholm C, Hallberg P, Sundqvist S, Lyngfelt A. Chemical-Looping Combustion of Solid Fuels Using Manganese Ores as Oxygen Carriers. Energy Fuels 2016;30:1204-16.

[12] Abad A, Gayán P, Mendiara T, Bueno J A, García-Labiano F, de Diego L F, Adánez J. Assessment of the improvement of chemical looping combustion of coal by using a manganese ore as oxygen carrier. Fuel Process Technol 2018;176:107-18.

[13] Schmitz M, Linderholm C. Chemical looping combustion of biomass in 10- and 100-kW pilots - Analysis of conversion and lifetime using a sintered manganese ore. Fuel 2018;231:73-84.

[14] Sundqvist S, Khalilian N, Leion H, Mattisson T, Lyngfelt A. Manganese ores as oxygen carriers for chemical-looping combustion (CLC) and chemical-looping with oxygen uncoupling (CLOU). Journal of Environmental Chemical Engineering 2017;5:2552-63.

[15] Niu X, Shen L, Gu H, Jiang S, Xiao J. Characteristics of hematite and fly ash during chemical looping combustion of sewage sludge. Chem Eng J 2015;268:236-44.

[16] Mendiara T, Pérez-Astray A, Izquierdo M T, Abad A, de Diego L F, García-Labiano F, Gayán P, Adánez J. Chemical Looping Combustion of different types of biomass in a 0.5 kW_{th} unit. Fuel 2018;211:868-75.

[17] Mendiara T, García-Labiano F, Abad A, Gayán P, de Diego L F, Izquierdo M T, Adánez J. Negative CO_2 emissions through chemical looping technology. Appl Energ 2018;232:657-84.

[18] Pikkarainen T, Hiltunen I. In: Chemical looping combustion of solid biomass - Performance of ilmenite and braunite as oxygen carrier materials, Eur. Biomass Conf. Exhib. Proc. , Stockholm, Sweden, 2017; Stockholm, Sweden, pp 1837-44.

[19] Mei D, Mendiara T, Abad A, de Diego L F, García-Labiano F, Gayán P, Adánez J, Zhao H. Evaluation of Manganese Minerals for Chemical Looping Combustion. Energy Fuels 2015;29:6605-15.

[20] Mei D, Mendiara T, Abad A, de Diego L F, García-Labiano F, Gayán P, Adánez J, Zhao H. Manganese Minerals as Oxygen Carriers for Chemical Looping Combustion of Coal. Ind Eng Chem Res 2016;55:6539-46.

[21] International Olive Oil Council, http://www.internationaloliveoil.org. (May 2, 2019),

[22] International Nut and dried Fruit. http://www.nutfruit.org (May 2, 2019),

[23] Simell P, Ståhlberg P, Kurkela E, Albrecht J, Deutsch S, Sjöström K. Provisional protocol for the sampling and anlaysis of tar and particulates in the gas from large-scale biomass gasifiers. Version 1998. Biomass Bioenergy 2000;18:19-38.

[24] Gayán P, Abad A, de Diego L F, García-Labiano F, Adánez J. Assessment of technological solutions for improving chemical looping combustion of solid fuels with CO_2 capture. Chem Eng J 2013;233:56-69.

[25] Haus J, Feng Y, Hartge E U, Heinrich S, Werther J. In: High volatiles conversion in a dual stage fuel reactor system for Chemical Looping Combustion of wood biomass, International Conference on Negative CO_2 emissions, Göteborg (Sweden), 2018; Göteborg (Sweden).

[26] Yan J, Shen L, Jiang S, Wu J, Shen T, Song T. Combustion Performance of Sewage Sludge in a Novel CLC System with a Two-Stage Fuel Reactor. Energy Fuels 2017;31:12570-81.

[27] Jiang S, Shen L, Yan J, Ge H, Song T. Performance in Coupled Fluidized Beds for Chemical Looping Combustion of CO and Biomass Using Hematite as an Oxygen Carrier. Energy Fuels 2018;32:12721-9.

[28] Pérez-Astray A, Adánez-Rubio I, Mendiara T, Izquierdo M T, Abad A, Gayán P, de Diego L F, García-Labiano F, Adánez J. Comparative study of fuel-N and tar evolution in chemical looping combustion of biomass under both iG-CLC and CLOU modes. Fuel 2019;236:598-607.

[29] de Visser E, Hendriks C, Barrio M, Mølnvik M J, de Koeijer G, Liljemark S, Le Gallo Y. Dynamis CO_2 quality recommendations. Int J Greenh Gas Con 2008;2:478-84.